LETTER

MOLECULAR TARGETS FOR THERAPY

CRISPR screening in human hematopoietic stem and progenitor cells reveals an enrichment for tumor suppressor genes within chromosome 7 commonly deleted regions

Jeremy T. Baeten[1,2], Weihan Liu[1,2], Isabelle C. Preddy[1,2], Ningxuan Zhou[3] and Megan E. McNerney[1,2]✉

Leukemia; https://doi.org/10.1038/s41375-021-01491-z

TO THE EDITOR:

Monosomy 7 and del(7q) are adverse-risk cytogenetic abnormalities prevalent in myeloid malignancies in both pediatric and adult acute myeloid leukemia (AML) and myelodysplastic syndrome (MDS) [1]. −7 and del(7q) are detected in clonal hematopoiesis and can be initiating events in transformation [2, 3]. Despite its clear clinical import, the underlying mechanism by which −7/del(7q) promotes transformation is incompletely understood. It has been postulated that critical tumor suppressor genes (TSGs) are encoded on chromosome 7, however identifying these genes has been challenging. Approaches have included mapping commonly deleted regions (CDRs), which helped identify *CUX1* [4], and searching for second-hit mutations, which pinpointed *EZH2* [5]. Large-scale cancer re-sequencing has shown that, with the exception of *EZH2* and *CUX1*, recurrent somatic mutations in chromosome 7 genes are rare. Here we implement in silico and in vitro screening as an alternative means to systematically uncover latent chromosome 7 TSGs.

To identify potential chromosome 7 TSGs in an unbiased manner, we mined genome-wide proliferation screens using CRISPR, gene-trap, and cDNA libraries performed in hematopoietic and non-hematopoietic cells. Thresholds for inclusion were set based on increased growth/selection in essential gene screens (CRISPRko, CRISPRi, and gene-trap) or decreased growth/selection in overexpression screens (CRISPRa and cDNA libraries). Overlap between multiple studies was prioritized, but thresholds were not stringent to cast a wide net for inclusion in further testing. We also included TSGs predicted from pan-cancer analyses of mutational patterns across thousands of primary patient cancers and TSGs from the Cancer Gene Census list. From these 12 datasets, we identified 96 coding genes with evidence of TSG activity that are also expressed in human HSPCs (Supplementary Table 1). For completeness, we also included all HSPC-expressed coding genes within the CDRs of 7q (q21.3, q22.1, q34, and q35–36), resulting in a total of 161 genes (Fig. 1A).

We next functionally tested the impact of editing the candidate genes in primary, human CD34+ HSPCs. We reasoned that deletion of putative TSGs would increase hematopoietic stem and progenitor cell (HSPC) proliferation and/or impair erythroid differentiation, both features of AML and myelodysplastic syndrome, respectively [6]. We chose an array-based CRISPR screen in lieu of a pooled approach for increased power to detect these features [7] (Fig. 1B). We transfected Cas9-gRNA ribonucleoprotein complexes into CD34+ HSPCs in a 96-well format, with one gRNA per gene per well. Two parallel screens were performed: (i) cells were cultured in maintenance media to assess HSPC proliferation, and (ii) cells were cultured in EPO-containing media to promote erythroid differentiation (see Supplementary Methods). *AAVS1* gRNA was used as a negative control, gPTEN was included as a positive control for increased proliferation, and gGATA1 was used as a control for decreased differentiation (Supplementary Fig. 1). Each gRNA was tested in 3–4 biological replicates with 108 guides (excluding controls) passing a threshold of >25% mean editing across all replicates, with a final mean editing efficiency of 47.9% (Fig. 1C). We chose this threshold with the assumption that knockout of a TSG causes edited cell outgrowth, which was borne out (Supplementary Fig. 2). We selected day 5 for proliferation measurements as that time point showed the greatest separation of genes without a plateau due to well overgrowth (Supplementary Fig. 3). Overall, replicates in both the proliferation and differentiation assay were well correlated (Supplementary Figs. 4, 5, 6).

Thirty-nine percent (42/108) of target genes significantly increased proliferation when edited (Fig. 1D). Only two genes, *CUX1* and *ACHE*, had a significant impairment of erythroid differentiation (Fig. 1E). This indicates that *CUX1* and *ACHE* may play a major role in differentiation defects in −7/del(7q)-associated myeloid malignancies. Across all genes, accelerated proliferation correlated with impaired erythropoiesis, consistent with the known link between these two processes (Fig. 1F). Using a combined proliferation and erythroid impairment metric (see Methods), twelve target genes scored significantly different from gAAVS1 ($p < 0.05$; FDR < 0.12, red circles, Fig. 1F). Nine of the twelve genes are within the CDRs and six encode DNA binding proteins; several of these have known roles in the regulation of proliferation while others are less well characterized (further discussed in Supplementary Note).

[1]Department of Pathology, The University of Chicago Medicine Comprehensive Cancer Center, The University of Chicago, Chicago, IL, USA. [2]Department of Pediatrics, Section of Hematology/Oncology, The University of Chicago Medicine Comprehensive Cancer Center, The University of Chicago, Chicago, IL, USA. [3]Department of Molecular and Cell Biology, University of California, Berkeley, CA, USA. ✉email: megan.mcnerney@uchospitals.edu

Received: 25 April 2021 Revised: 22 November 2021 Accepted: 1 December 2021
Published online: 17 January 2022

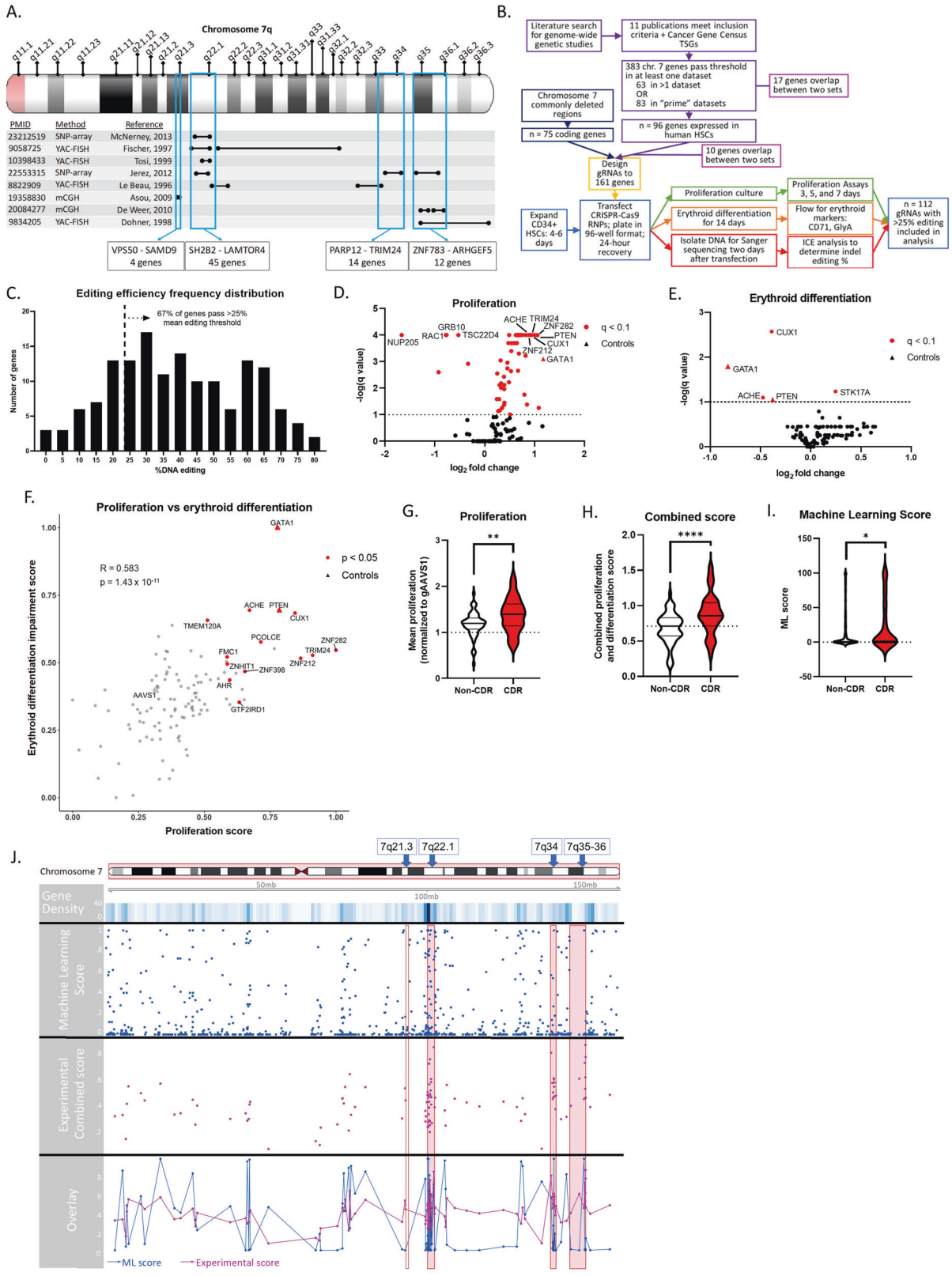
A.
Chromosome 7q
PMID Method Reference
23212519 SNP-array McNerney, 2013
9058725 YAC-FISH Fischer, 1997
10398433 YAC-FISH Tosi, 1999
22553315 SNP-array Jerez, 2012
8822909 YAC-FISH Le Beau, 1996
19358830 mCGH Asou, 2009
20084277 mCGH De Weer, 2010
9834205 YAC-FISH Dohner, 1998
VPS50 - SAMD9 4 genes
SH2B2 - LAMTOR4 45 genes
PARP12 - TRIM24 14 genes
ZNF783 - ARHGEF5 12 genes
B.
Literature search for genome-wide genetic studies
11 publications meet inclusion criteria + Cancer Gene Census TSGs
383 chr. 7 genes pass threshold in at least one dataset 63 in >1 dataset OR 83 in "prime" datasets
17 genes overlap between two sets
Chromosome 7 commonly deleted regions
n = 75 coding genes
n = 96 genes expressed in human HSCs
10 genes overlap between two sets
Design gRNAs to 161 genes
Expand CD34+ HSCs: 4-6 days
Transfect CRISPR-Cas9 RNPs; plate in 96-well format; 24-hour recovery
Proliferation culture
Erythroid differentiation for 14 days
Isolate DNA for Sanger sequencing two days after transfection
Proliferation Assays 3, 5, and 7 days
Flow for erythroid markers: CD71, GlyA
ICE analysis to determine indel editing %
n = 112 gRNAs with >25% editing included in analysis
C.
Editing efficiency frequency distribution
67% of genes pass >25% mean editing threshold
Number of genes
%DNA editing
D.
Proliferation
-log(q value)
log2 fold change
q < 0.1
Controls
E.
Erythroid differentiation
-log(q value)
log2 fold change
q < 0.1
Controls
F.
Proliferation vs erythroid differentiation
R = 0.583
p = 1.43 x 10-11
p < 0.05
Controls
Erythroid differentiation impairment score
Proliferation score
G.
Proliferation
Mean proliferation (normalized to gAAVS1)
Non-CDR
CDR
H.
Combined score
Combined proliferation and differentiation score
Non-CDR
CDR
I.
Machine Learning Score
ML score
Non-CDR
CDR
J.
Chromosome 7
7q21.3
7q22.1
7q34
7q35-36
Gene Density
Machine Learning Score
Experimental Combined score
Overlay
ML score
Experimental score

Fig. 1 Arrayed CRISPR-Cas9 screen and machine learning classification identify multiple chromosome 7 genes with myeloid tumor suppressor activity, concentrated within 7q CDRs. A Graphic depicting the selection of previously defined CDRs in chromosome 7q. Black bars indicate regions identified by each publication; blue boxes are the regions included in this study. YAC–FISH: Yeast artificial chromosome–fluorescence in situ hybridization, SNP-array: single nucleotide polymorphism array, mCGH microarray: comparative genomic hybridization. **B** Flow chart describing the arrayed CRISPR-Cas9 screen experimental design. "Prime" datasets were defined as those with complete statistical data available and performed in AML cell lines. **C** Mean editing percentages of each gene targeted by a single gRNA across replicates, shown as a frequency distribution. Dotted line indicates 25% threshold required for inclusion in analysis, with 67% of gRNAs included. **D**, **E** Volcano plots depicting $\log_2$ fold change (to gAAVS1 control) and −log q value of day 5 proliferation assays (**D**; $n = 7$) and day 14 erythroid differentiation assays (**E**; $n = 8$). Each dot is the mean value of a gene across replicates; controls denoted by a triangle; red indicates statistical significance determined by Dunnett multiple comparisons test for proliferation and multiple *t* tests for erythroid differentiation, $q < 0.1$. **F** Proliferation and erythroid differentiation values were scaled to fall between 0 and 1, and the erythroid sign inverted so that a higher score is associated with increased proliferation and decreased erythroid differentiation. Each dot is the mean value of a gene across replicates; controls denoted by a triangle; red indicates statistical significance determined by Mann–Whitney–Wilcoxon test on summed proliferation and erythroid differentiation impairment scores, $p < 0.05$, $q < 0.12$. Correlation statistics calculated with Pearson R value and student *t* test *p* value. **G** Proliferation normalized to gAAVS1 or (**H**) combined score of genes within commonly deleted regions of 7q compared to those outside. Significance determined by student *t* test, $^*p < 0.05$; $^{**}p < 0.01$; $^{***}p < 0.001$. $n = 59$ non-CDR genes; $n = 53$ CDR genes. **I** Machine learning score of genes within ($n = 74$) or outside of CDRs ($n = 825$). Significance determined by Mann–Whitney–Wilcoxon test, $^*p < 0.05$. **J** Genomic track of all chromosome 7 genes. Rows depict gene density, machine learning score, combined proliferation and erythroid differentiation score, and overlay of machine learning (ML) and experimental scores. Red boxes indicate CDRs.

Across all genes, the effect on proliferation was non-random, with a significant bias towards increased proliferation (Supplementary Fig. 7). This is perhaps a consequence of, and affirms, our inclusion criteria (Fig. 1A). The effect size for genes within CDRs was significantly more pronounced, as measured by either proliferation alone (Fig. 1G) or through the combined score (Fig. 1H). This result is remarkable because while the other genes in the screen were pre-selected for by their performance in other CRISPR screens, all CDR genes were included, regardless of previous evidence of TSG activity. That the CDR regions are significantly enriched for TSGs implies that the deletion of these regions in myeloid malignancies contributes to disease progression through the combined loss of several contributing genes.

We next sought to validate and extend our finding of increased TSGs within CDRs through an orthogonal approach assessing all chromosome 7 coding genes. In recent years, machine learning has proved a powerful tool in uncovering biological associations hidden in large datasets [8]. We implemented a random forest classification model using eight cancer genome-wide screens and one mutational signature dataset spanning 24 different cell lines to assign a TSG score for each gene (Supplementary Figs. 8, 9). We created training and testing datasets from all protein coding genes outside of chromosome 7 using the bootstrap method and used canonical TSGs curated from Cancer Gene Census as the ground truth for our training process. The performance of the classification system was strong, yielding an average AUC of 0.777 [0.747–0.806, 95% CI]). We then ran the classifier on chromosome 7 genes, and many highly scoring genes overlapped with genes that scored significantly experimentally, such as *CUX1, LUC7L2* [9], and *TRIM24* [10] (Supplementary Fig. 10). The overlap of the experimental and classifier results did not reach significance (hypergeometric test $p = 0.12$). Conceivably, this may reflect a limitation of the classifier and/or some hits in the classifier may exhibit tumor suppressor activity by other measurements, such as apoptosis, metastasis, or DNA repair. Nonetheless, using the classifier scores, genes within CDRs are again significantly enriched for TSGs (Fig. 1I, J). This result from disparate datasets, across tumor types, mirrors our experimental results. To our knowledge, the successful application of machine learning with genomic and CRISPR screen data to identify TSGs has not been previously reported. Furthermore, our result buttresses the concept of CDRs manifesting as a contiguous gene syndrome.

As *CUX1* and *ACHE* were the only genes with significant experimental effects on both proliferation and differentiation (by non-combined metrics), we chose these candidates for further investigation. We validated our findings with independent gRNAs targeting *CUX1* and *ACHE*. All gRNAs decreased protein levels (Fig. 2A, D) and recapitulated the proliferation and erythroid differentiation phenotypes seen in the screen (Fig. 2B, C and G, H). These *CUX1* results are consistent with the HSPC proliferation and anemia we observed in CUX1-knockdown mice [11]. *ACHE* is located with *CUX1* in the 7q22.1 CDR and encodes extracellular membrane-associated acetylcholinesterase, also known as the Cartwright blood group. In neuromuscular junctions, acetylcholinesterase degrades acetylcholine to abrogate acetylcholine receptor signaling [12], however the hematopoietic function of *ACHE* is unknown. We tested the effect of the muscarinic acetycholine receptor inhibitor, oxyphenonium bromide, and found that it had the opposite effect of loss of *ACHE*, causing decreased proliferation and increased erythroid differentiation (Fig. 2E, F). Importantly, oxyphenonium bromide treatment in gACHE cells restored proliferation and differentiation to the same level as the gAAVS1 control (Fig. 2G, H). This is congruent with a model wherein loss of *ACHE* in HSPCs causes increased muscarinic acetylcholine receptor signaling, leading to increased proliferation and impaired erythroid differentiation, contributing to the myeloid expansion and anemia seen in −7/del7q myeloid malignancies (Fig. 2I). As multiple muscarinic antagonists are FDA-approved or in clinical trials, this may be a feasible treatment avenue for anemia associated with −7/del (7q) myeloid disease.

Overall, our study identifies several potential chromosome 7 TSGs and demonstrates that TSG activity is enriched within the 7q CDRs. While *CUX1* and *ACHE* exert the strongest TSG phenotypes, combinatorial loss of multiple genes may characterize a contiguous gene syndrome in the leukemogenesis of monosomy 7.

A limitation of our study is that 33% of the tested genes have been excluded from our analysis due to either inefficient transfection or gRNA editing in some cases. Some of these genes have been reported to display TSG activity, including *EZH2* [5] and *KMT2C* [13], which also score highly by our machine learning classifier, and *KMT2E* [14] and *SAMD9* [15]. Thus, we cannot rule out a role for the excluded genes. *SAMD9L* [15] was included in our analysis but did not score highly as a TSG in the CRISPR screen or by machine learning. Due to the shorter duration of the proliferation assay, rare proteins with particularly long half-lives may present as false negatives. Another limitation is that gRNAs generate both heterozygous and homozygous editing; further experiments determining the haploinsufficient nature of these putative TSGs is warranted.

Overall, we demonstrate that datamining and machine learning with existing genome-wide datasets is a high-yield approach to dissecting the pathogenesis of recurrent, chromosome arm-level aneuploidies in cancer.

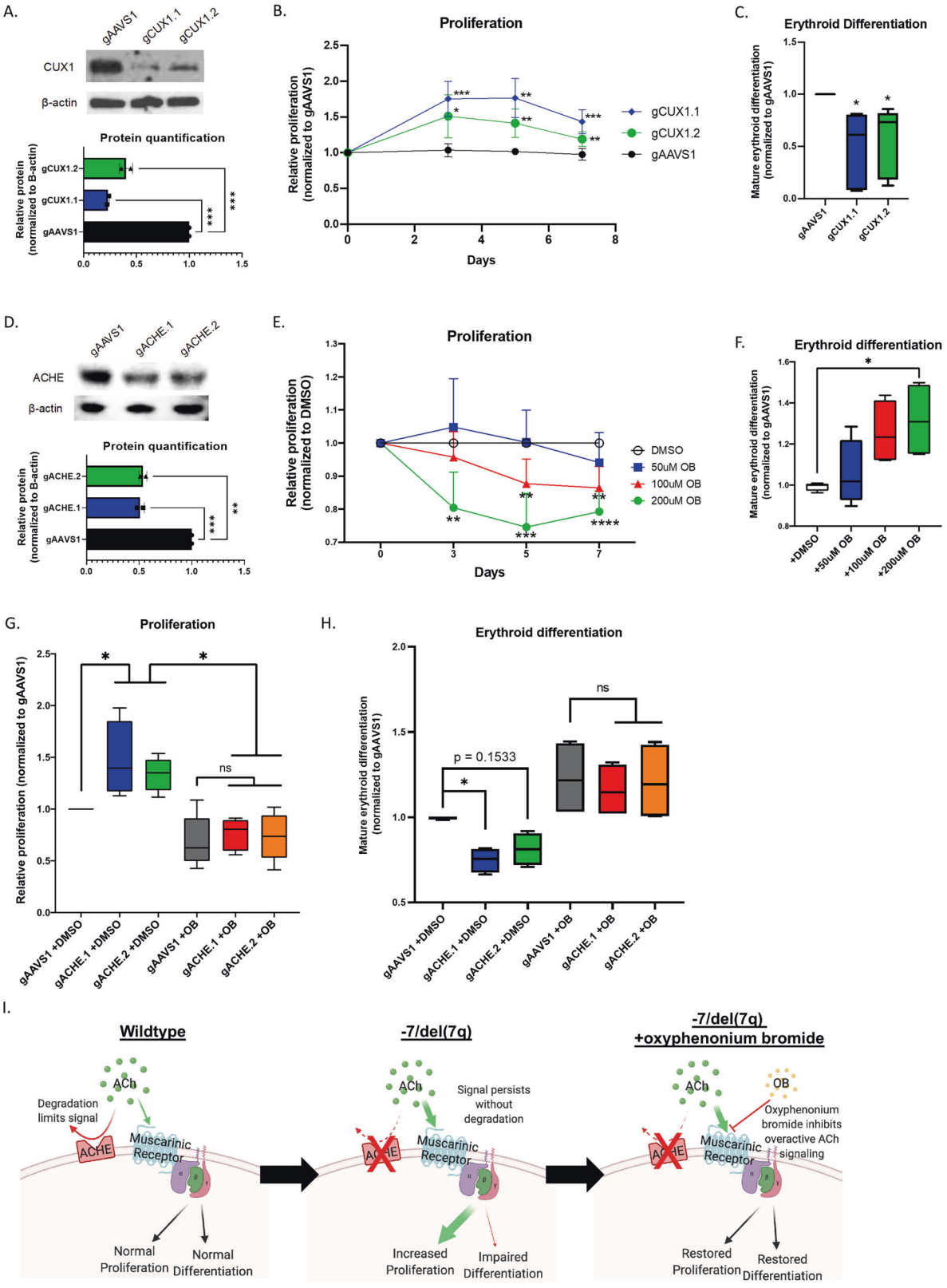
A.
gAAVS1
gCUX1.1
gCUX1.2
CUX1
β-actin
Protein quantification
Relative protein (normalized to B-actin)
gCUX1.2
gCUX1.1
gAAVS1
B.
Proliferation
Relative proliferation (normalized to gAAVS1)
Days
gCUX1.1
gCUX1.2
gAAVS1
C.
Erythroid Differentiation
Mature erythroid differentiation (normalized to gAAVS1)
gAAVS1
gCUX1.1
gCUX1.2
D.
gAAVS1
gACHE.1
gACHE.2
ACHE
β-actin
Protein quantification
Relative protein (normalized to B-actin)
gACHE.2
gACHE.1
gAAVS1
E.
Proliferation
Relative proliferation (normalized to DMSO)
Days
DMSO
50uM OB
100uM OB
200uM OB
F.
Erythroid differentiation
Mature erythroid differentiation (normalized to gAAVS1)
+DMSO
+50uM OB
+100uM OB
+200uM OB
G.
Proliferation
Relative proliferation (normalized to gAAVS1)
ns
gAAVS1 +DMSO
gACHE.1 +DMSO
gACHE.2 +DMSO
gAAVS1 +OB
gACHE.1 +OB
gACHE.2 +OB
H.
Erythroid differentiation
Mature erythroid differentiation (normalized to gAAVS1)
p = 0.1533
ns
gAAVS1 +DMSO
gACHE.1 +DMSO
gACHE.2 +DMSO
gAAVS1 +OB
gACHE.1 +OB
gACHE.2 +OB
I.
Wildtype
ACh
Degradation limits signal
ACHE
Muscarinic Receptor
Normal Proliferation
Normal Differentiation
-7/del(7q)
ACh
Signal persists without degradation
Muscarinic Receptor
Increased Proliferation
Impaired Differentiation
-7/del(7q) +oxyphenonium bromide
ACh
OB
Oxyphenonium bromide inhibits overactive ACh signaling
Muscarinic Receptor
Restored Proliferation
Restored Differentiation

Fig. 2 *CUX1* and *ACHE* are potential TSGs in the 7q22.1 CDR, and *ACHE* loss can be rescued by a muscarinic acetylcholine inhibitor. **A** Representative western blot of p200 CUX1 protein knockdown in human CD34+ cells 3 days after transfection with two different gRNAs. β-actin loading control. Relative protein quantified by densitometry, significance determined by one-way ANOVA and Dunnett's multiple comparisons test, $n = 2$. *$p < 0.05$; **$p < 0.01$; ***$p < 0.001$. **B** Proliferation time course normalized to gAAVS1. Significance determined by 2-way repeated measures ANOVA with Geisser-Greenhouse correction and Dunnett's multiple comparisons test, $n = 6$. *$p < 0.05$; **$p < 0.01$; ***$p < 0.001$. **C** gAAVS1 normalized mature/total erythroid differentiation ratio, determined by flow for CD71 and GlyA markers after 14 days in culture. Significance determined by paired *t* test, $n = 5$. **D** Representative western blot of ACHE protein knockdown 3 days after transfection with two different gRNAs. β-actin loading control. Relative protein quantified by densitometry, significance determined by one-way ANOVA and Dunnett's multiple comparisons test, $n = 2$. *$p < 0.05$; **$p < 0.01$; ***$p < 0.001$. **E** Proliferation time course after treatment with muscarinic acetylcholine receptor inhibitor oxyphenonium bromide, normalized to DMSO vehicle control. Significance determined by 2-way repeated measures ANOVA with Geisser-Greenhouse correction and Dunnett's multiple comparisons test, $n = 4$. *$p < 0.05$; **$p < 0.01$; ***$p < 0.001$. **F** gAAVS1 normalized mature/total erythroid differentiation ratio after 14 days in culture. Significance determined by one-way ANOVA and Dunnett's multiple comparisons test, $n = 4$. **G** 5-day proliferation and (**H**) 14-day mature/total erythroid differentiation ratio normalized to gAAVS1 with *ACHE* gRNAs and/or 200 μM oxyphenonium bromide. Significance determined by one-way ANOVA and Tukey's multiple comparisons test, $n = 4$. **I** Graphic depicting the proposed model for the impact of ACHE loss in CD34+ cells. When ACHE is present on the cell surface, acetylcholine (ACh) signaling through muscarinic acetylcholine receptors is limited in duration and/or magnitude. Without ACHE, the ACh signal persists and leads to increased proliferation and impaired erythroid differentiation. Treatment with the oxyphenonium (OB) inhibitor blocks aberrant ACh signal and restores CD34+ cell to a normal level of proliferation and erythroid differentiation. *$p <$ 0.05; **$p < 0.01$; ***$p < 0.001$; ****$p < 0.0001$; ns not significant, ACHE acetylcholinesterase, ACh acetylcholine, OB oxyphenonium bromide.

REFERENCES

1. Inaba T, Honda H, Matsui H. The enigma of monosomy 7. Blood. 2018;131:2891–8. https://doi.org/10.1182/blood-2017-12-822262.
2. Takahashi K, Wang F, Kantarjian H, Song X, Patel K, Neelapu S, et al. Copy number alterations detected as clonal hematopoiesis of indeterminate potential. Blood Adv. 2017;1:1031–6. https://doi.org/10.1182/bloodadvances.2017007922.
3. Dimitriou M, Woll PS, Mortera-Blanco T, Karimi M, Wedge DC, Doolittle H, et al. Perturbed hematopoietic stem and progenitor cell hierarchy in myelodysplastic syndromes patients with monosomy 7 as the sole cytogenetic abnormality. Oncotarget. 2016;7:72685–98. https://doi.org/10.18632/oncotarget.12234.
4. McNerney ME, Brown CD, Wang X, Bartom ET, Karmakar S, Bandlamudi C, et al. CUX1 is a haploinsufficient tumor suppressor gene on chromosome 7 frequently inactivated in acute myeloid leukemia. Blood. 2013;121:975–83. https://doi.org/10.1182/blood-2012-04-426965.
5. Ernst T, Chase AJ, Score J, Hidalgo-Curtis CE, Bryant C, Jones AV, et al. Inactivating mutations of the histone methyltransferase gene EZH2 in myeloid disorders. Nat Genet. 2010;42:722–6. https://doi.org/10.1038/ng.621.
6. Ebert BL, Pretz J, Bosco J, Chang CY, Tamayo P, Galili N, et al. Identification of RPS14 as a 5q- syndrome gene by RNA interference screen. Nature. 2008;451:335–9. https://doi.org/10.1038/nature06494.
7. Shalem O, Sanjana NE, Zhang F. High-throughput functional genomics using CRISPR-Cas9. Nat Rev Genet. 2015;16:299–311. https://doi.org/10.1038/nrg3899.
8. Camacho DM, Collins KM, Powers RK, Costello JC, Collins JJ. Next-generation machine learning for biological networks. Cell. 2018;173:1581–92. https://doi.org/10.1016/j.cell.2018.05.015.
9. Makishima H, Visconte V, Sakaguchi H, Jankowska AM, Abu Kar S, Jerez A, et al. Mutations in the spliceosome machinery, a novel and ubiquitous pathway in leukemogenesis. Blood. 2012;119:3203–10. https://doi.org/10.1182/blood-2011-12-399774.
10. Tisserand J, Khetchoumian K, Thibault C, Dembélé D, Chambon P, Losson R. Tripartite motif 24 (Trim24/Tif1α) tumor suppressor protein is a novel negative regulator of interferon (IFN)/signal transducers and activators of transcription (STAT) signaling pathway acting through retinoic acid receptor α (Rarα) inhibition. J Biol Chem. 2011;286:33369–79. https://doi.org/10.1074/jbc.M111.225680.
11. An N, Khan S, Imgruet MK, Gurbuxani SK, Konecki SN, Burgess MR, et al. Gene dosage effect of CUX1 in a murine model disrupts HSC homeostasis and controls the severity and mortality of MDS. Blood. 2018;131:2682–97. https://doi.org/10.1182/blood-2017-10-810028.
12. Taylor P, Radić Z. The cholinesterases: from genes to proteins. Annu Rev Pharmacol Toxicol. 1994;34:281–320. https://doi.org/10.1146/annurev.pa.34.040194.001433.
13. Chen C, Liu Y, Rappaport AR, Kitzing T, Schultz N, Zhao Z, et al. MLL3 is a haploinsufficient 7q tumor suppressor in acute myeloid leukemia. Cancer Cell. 2014;25:652–65. https://doi.org/10.1016/j.ccr.2014.03.016.
14. Zhang Y, Wong J, Klinger M, Tran MT, Shannon KM, Killeen N. MLL5 contributes to hematopoietic stem cell fitness and homeostasis. Blood. 2009;113:1455–63. https://doi.org/10.1182/blood-2008-05-159905.
15. Davidsson J, Puschmann A, Tedgård U, Bryder D, Nilsson L, Cammenga J. SAMD9 and SAMD9L in inherited predisposition to ataxia, pancytopenia, and myeloid malignancies. Leukemia. 2018;32:1106–15. https://doi.org/10.1038/s41375-018-0074-4.

ACKNOWLEDGEMENTS

The authors are grateful for the services and assistance provided by University of Chicago core facilities supported by the Cancer Center Support Grant (P30 CA014599). In particular, the authors thank William Buikema and the DNA Sequencing and Genotyping Facility Core for special assistance and services (RRID:SCR_019196). We also acknowledge support from the Cytometry and Antibody Technology Core (RRID: SCR_017760) and the Center for Research Informatics Bioinformatics Core.

AUTHOR CONTRIBUTIONS

JTB and ICP performed experiments and datamining; WL and SZ performed machine learning analysis; JTB and WL analyzed results and made the figures; JTB, WL, and MEM designed the research and wrote the paper.

FUNDING

This work was funded in part by NIH/NHLBI R01 HL142782, NIH/NCI R01 CA231880, American Cancer Society Research Scholar Award 132457-RSG-18-171-01-LIB, American Society of Hematology Junior Faculty Scholar Award, the Brinson Foundation, and The University of Chicago Cancer Research Foundation Women's Board. The authors gratefully acknowledge the support of Robin and Matthew Patinkin.

COMPETING INTERESTS

The authors declare no competing interests.

ADDITIONAL INFORMATION

Supplementary information The online version contains supplementary material available at https://doi.org/10.1038/s41375-021-01491-z.

Correspondence and requests for materials should be addressed to Megan E. McNerney.

Reprints and permission information is available at http://www.nature.com/reprints

Publisher's note Springer Nature remains neutral with regard to jurisdictional claims in published maps and institutional affiliations.